Sea Breeze Interactions with Aerosol Content and Atmospheric Boundary Layer Structure in the Coastal Houston Region

Isaac Medina*

Johns Hopkins University, Baltimore, Maryland

ABSTRACT

Surface based aerosol emissions that could impact human health can often become trapped within and mixed into the Atmospheric Boundary Layer (ABL) (Miller et al. 2003). Therefore, understanding how mesoscale phenomenon, like the sea breeze (SB), effect this entrapment, can lead to better modeling and improved forecasting. To facilitate this idea, we use data from the Tracing Aerosol Convection Interactions Experiment (TRACER) project which took place in Houston, TX in 2022. We compare aerosol content data prior to and post SB passage for singular and consecutive SB cases. Here we observe a considerable increase in aerosol content post SB passage when compared to earlier in the day, and against the same time of day on days without SB passage. For consecutive cases we also observe a general increase in aerosol content with day, with a particular spike in aerosol content around sunrise for days 2-6. However, without more consecutive SB cases it is hard to determine if this is a direct result of recirculation or local anthropogenic changes. We also observe boundary layer structure changes consistent with prior literature, including the lowering of the daytime ABL height, and the suppression of vertical mixing, denoted by a decrease in vertical velocity variance. This suppression supports the notion that increases in surface-based aerosols may be due to both advection by the SB and the suppression of mixing of existing aerosol sources.

1. Introduction

The sea-breeze (SB) circulation can be a large contributor to pollution events as it can alter the structure of the atmospheric boundary layer (ABL), helping to lower the mixing height of the daytime convective boundary layer (CBL), in turn increasing near surface concentrations of emitted aerosols (Miller et al. 2003). Large cities that lie within coastal regions, like Houston, Texas, could therefore be at an elevated risk for such pollution events. This is especially concerning during the warm summer months, when SBs are more common and when pollution from nearby traditional energy generation sources may be higher as demand for air conditioning grows. Understanding how the SB interacts with aerosols in this region could then lead to better forecasting for such events.

The SB is a thermally direct circulation, in which a pressure differential forms from the differential surface heating across the land and a large nearby body of water (Physick and Byron-Scott 1977). Generally, this favors onshore flow during the day and offshore flow during the night, most notably during relatively calm synoptic conditions, in which no strong background pressure gradients are present to dominate the local dynamics (Physick and Byron-Scott 1977). The SB's diurnal oscillation between on and offshore flow can lead to an increase in aerosol recirculation as land-based pollutants are carried out onto the water overnight, then back onto land the next day by the SB (Physick and Byron-Scott 1977; Parajuli et al. 2020). This recirculation, as hypothesized by Physick and Byron-Scott (1977) could lead to local air quality events if the SB dominates the local dynamics for multiple days in a row.

The passage of the SB has long been correlated with a local increase in aerosol content (Physick and Byron-Scott 1977; Moorthy et al. 1993; Talbot et al. 2007; Augustin et al. 2020; Parajuli et al. 2020). Particularly studies have found increases in $PM_{2.5}$, and NO_x (Augustin et al. 2020) and small ($< 0.28\mu m$) organic particles (Parajuli et al. 2020). Additionally, wind tunnel experiment by Ohba et al. (1998) found that that larger velocity variances directly resulted in lower ground concentrations. Thus, if the passage of the SB is suppressing vertical buoyant mixing, we should also expect lower variances and higher aerosol concentrations (Dewani et al. 2023).

These studies have also extended to include investigations into the Houston area. The area's pollutant circulation has been investigated by Chen et al. (2011) who used the Advanced Research Weather Research and Forecasting (ARW-WRF) model with a coupled urban canopy model to compare wind and temperature data to sparse measurements from around the Houston area and satellites. They found that while their model was well calibrated in these variables, they stress that further field campaigns are needed to understand and quantify the complex thermodynamic interplay between Houston and the gulf in the summertime can lead to stagnant flow events impacting air quality (Chen et al. 2011).

*Corresponding author: Isaac Medina, imedin2@jh.edu

In 2022, the Tracing Aerosol Convection Interactions Experiment (TRACER) field campaign was conducted to investigate how the SB circulation impacts convective initiation, aerosol transport, and the urban environment (Jensen et al. 2023; Klein et al. 2023). This campaign included multiple collaborators with different instrument suites across the greater Houston area.

Lappin et al. (2025) used the TRACER dataset to investigate the effects of the SB on the thermodynamic structure of the ABL. Although they mention that typically we would expect cooling and moistening from SB passage, this was not always present in this area (Lappin et al. 2025). They note that the lack of traditional SB effects on the thermodynamics meant that there was not an appreciable increase in surface stability (Lappin et al. 2025). Without the traditional increase in stability expected from the SB passage, it will be important to investigate how the SB in Houston interacts with the aerosol transport and recirculation that was seen in other studies.

In addition to this study, Wang et al. (2025) used the TRACER dataset and aerosol measurements from the Atmospheric Radiation Measurement (ARM) facility in La Porte, TX to investigate the impacts of aerosols on deep convective clouds. Along with their work to investigate cloud condensation nucelli (CCN) availability and content, they noted that they found multiple high pollution days in mid-July and mid-August (Wang et al. 2025). Thus we will be using the dataset from the La Porte site to investigate recirculation events in July.

2. Dataset

The primary data for this project was obtained from the main Atmospheric Radiation Measurement (ARM) facility in La Porte in Houston, TX (designated as ARM site AMF1) as part of TRACER in 2022. Due to data availability and the time constraints, only data from June and July 2022 were analyzed as a part of this project.

Horizontal wind speed and direction is derived from a scanning lidar, vertical wind speed is derived from lidar stares, the water vapor and temperature data is returned from a microwave radiometer (MWR), and the aerosol data is from a condensation particle counter (CPC) which has both 2.5nm and 10nm detection limits. For this project all of our aerosol data will be returned from the 2.5nm detection limit condensation particle counter to capture small particles that may be present from SB transport and recirculation (Parajuli et al. 2020).

3. Methodology

All code and data used for this project can be found on the GitHub site associated with this project, available in the *data availability statement* section.

Sea Breeze Identification

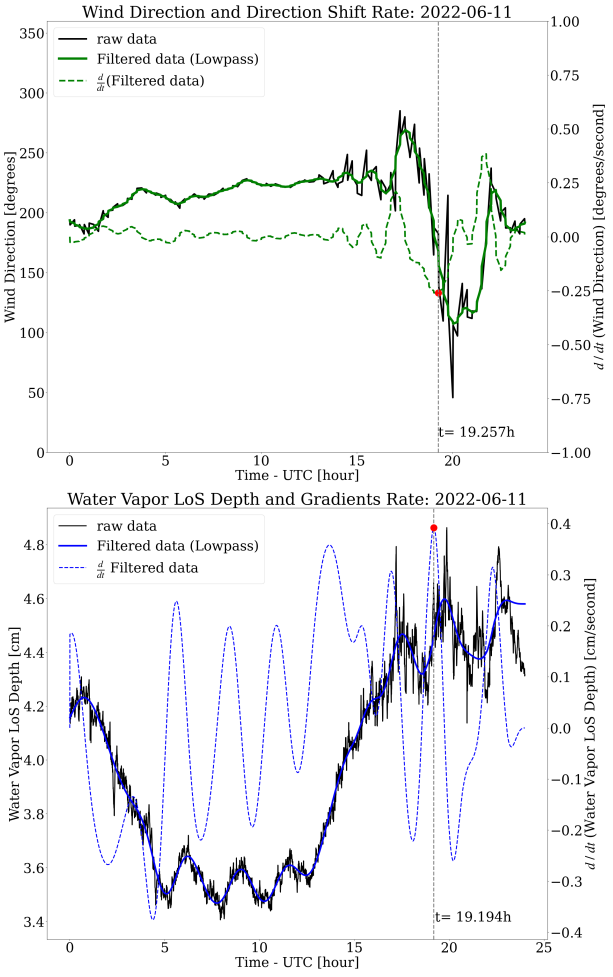

FIG. 1. Wind direction data (top) and Water Vapor (bottom) for June 11th 2022. On the top, the raw (black) and low-pass filtered (solid green) wind direction data is plotted with the first derivative in time (dashed green) with the minimum and associated time marked. On the bottom the raw (black) and low-pass filtered (solid blue) line of sight (LoS) water vapor data is plotted with the first derivative in time (dashed blue) with the maximum and associated time marked. Here we note that both the wind speed gradient minimum and water vapor gradient maximum occur at roughly the same time (19:30 UTC).

To quantify the impact of the SB on aerosol concentrations, we must first identify SB passage. For this, we identify a wind shift, and an increase in water vapor (Lappin et al. 2025). Given the geometry of the coastline at our observational site, we expect the wind direction to become shore perpendicular or East-Southeasterly from shore parallel or Southwesterly. For this we will identify gradients numerically in both water vapor and wind direction using a second order central differencing scheme prescribed as:

$$\frac{du}{dt} = \frac{(u_{i+1} - u_{i-1})}{2\Delta t} \tag{1}$$

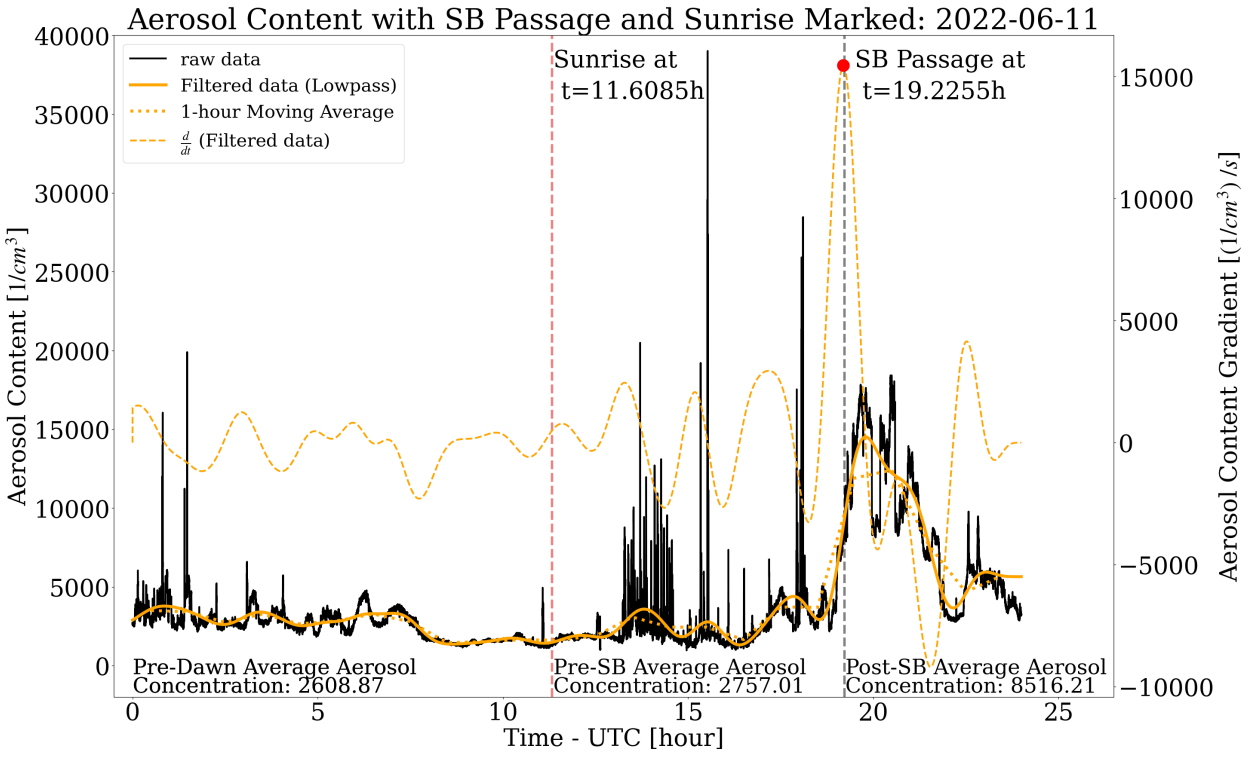

FIG. 2. Aerosol content data for June 11th 2022. The raw (black) and low-pass filtered (solid orange) aerosol content data is plotted with the first derivative in time (dashed orange). Here we note the time of SB passage as 19:13 UTC, calculated from wind speed and water vapor data (blue dashed) and sunrise (dashed red).

We then identify the largest increase in water vapor, and the largest negative change in wind direction (corresponding to winds backing to become southeasterly). Figure 1 demonstrates this process. While we traditionally also expect the SB to contribute to decreases in surface temperature, prior studies did not observe this affect in the Houston Area (Lappin et al. 2025). Thus, we did not use surface temperatures as a method for SB identification.

After the SB days were identified, the data was separated into three cases. These include clear days (with no SB), single SB days (days with SB passage without SB passage the day prior), and consecutive SB days (days with SB passage, that also had SB passage the day before). The consecutive SB cases will help give insight into estimated aerosol recirculation events. Here we did not distinguish between SB days that did or did not have convective initiation present.

TABLE 1. Case Days used for Data Anlysis

Case Type	Num. Cases	Dates
Clear	4	6/13, 6/14, 6/15, 7/20
Singular SB	4	6/11, 6/17, 6/23, 7/3
Consecutive SB	6	7/3, 7/4, 7/5, 7/6, 7/7, 7/8

Aerosol Correlation

Once SB passage is identified, we divide our aerosol data into three sections, pre-dawn, pre-SB, and post-SB, as seen in Fig 2. Firstly, splitting the data in to pre and post dawn allows for analysis of aerosol content to be quantified during the night when convective mixing is low, and the day when mixing is high. Secondly, we split the daytime into pre and post SB to quantify changes in aerosol content relative to SB passage. The data was also hourly averaged to quantify when a change in aerosol content change happened relative to SB passage time.

For non SB cases, we use the SB passage times from both singular and consecutive cases to obtain an average SB passage time to divide the daytime hours for cases that do not have an SB passage time of their own. This allows us to compare the aerosol content at relatively similar times of day to ensure any changes are due to SB passage and not local anthropogenic patterns.

Boundary Layer Height Identification

Here we use a modified version of the fuzzy-logic methodology developed by Smith and Carlin (2024). While this methodology was derived for the National Severe Storms Laboratory's (NSSL's) Collaborative Lower

Atmospheric Profiling System (CLAMPS), we will extend this to our available observational data, as CLAMPS features similar instruments and measurement techniques to what is available from the ARM-AMF1 site. For this we use horizontal and vertical motion retried from lidar data as well as thermodynamic data returned from the MWR.

Vertical Velocity Variance

During the computation of boundary layer height, the fuzzy-logic algorithm computes the vertical velocity variance (σ_w^2) as a function of time and height (Smith and Carlin 2024). As mentioned by Ohba et al. (1998), we may expect to see decreasing velocity variances with SB passage, thus to understand how SB passage affects vertical mixing within the ABL, we will use the calculated σ_w^2 to compare clear days with SB passage days.

For this we integrate the calculated σ_w^2 value over the estimated depth of the ABL. While σ_w^2 is used as one of the various inputs in the calculation of the ABL, such that lower σ_w^2 will lower the ABL height, the overall estimations of ABL height are not so different across the three cases that we would expect the depth of the column integrated to be a large factor impacting the value of σ_w^2. Thus, once integrated, we will have a quantification of σ_w^2 within the ABL as a function of time that we can use to compare the effects of SB passage on σ_w^2.

4. Results and Discussion

Aerosol Content

Despite the decreased correlation with increases in surface stability (Lappin et al. 2025), notable differences in aerosol content were still observed during days with SB passage. When compared to days without a SB, we see an increase in aerosol content in both single and consecutive SB days. We also do not see appreciable change in aerosol content during different times of day during non-SB cases except for slightly lower aerosol contents during daytime hours, likely due to increased mixing within the CBL.

Generally see an increase in aerosol content after the passage of the SB in both singular and consecutive SB cases. For the singular cases we also tend to see a greater decrease in aerosols overnight, though this trend is still partially present for the consecutive cases as well. This decrease may be a result of a land breeze pulling aerosols back out over the gulf, but more work would need to be done to identify the passage of such breeze in the kinematic and thermodynamic data.

In Fig. 3 we see an increase in aerosols in both consecutive and singular SB cases prior to the passage of the SB.For consecutive SBs this happens almost at sunrise, but the singular case happens much later, closer to the average SB passage time. The increase for in aerosols in the consecutive cases will be explored more in the following subsection. As the signal in the singular cases does not appear in the consecutive cases, we will look at each case individually to see where such an increase could originate, especially as the signal does not seem to appear in the bar graph either.

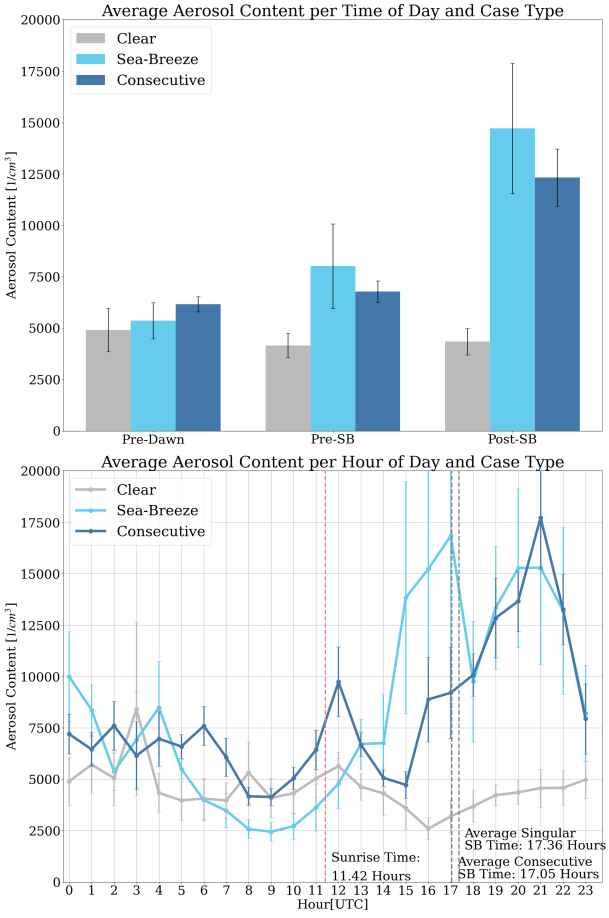

FIG. 3. Time of day (pre-dawn, pre-SB, post-SB) averaged aerosol content per case type (top), and hourly averaged aerosol content with error bars (bottom) for clear cases (grey) singular SB cases (light blue) and consecutive SB cases (dark blue). Error bars also noted in black on each bar (top) and respective case color (bottom). For the hourly averaged data the average time of SB passage from the associated dataset is noted and marked with a grey dashed line, and the sunrise time is noted and marked with a light red dashed line. Note that the error bars are much larger on the hourly averaged data for the singular cases, likely due to the large differences in SB passage, and thus the large differences in aerosol increase time.

When looking at each day individually, we found that for all cases the increase in aerosols happens at time of SB passage, or around 30 minutes either side of passage time. Thus, the peak in aerosol in the hourly data in Fig. 3 that appears to be before the average SB passage time, is an artifact of the different SB passage times across different days in our observational period. For cases with SB passage, Table 2 shows the time passage as well as aerosol content before, during, and after passage.

TABLE 2. SB passage time [UTC] and instantaneous aerosol content $[1/cm^3]$ for SB cases at time of passage and $\pm 1\ hr$.

Date	SB Time	−1 hr	±0 hr	+1 hr
6/11	19:13	3,674.339	9,337.124	13,069.722
6/17	16:13	11,430.569	26,964.578	10,136.6978
6/23	17:32	11,944.721	34,905.319	16,776.286
7/3	17:27	2,960.184	6,100.344	8,743.065
7/4	17:03	1,658.364	4,480.427	3,390.790
7/5	17:30	2,649.247	2,216.832	4,319.073
7/6	17:22	5,558.794	4,318.9267	8,774.429
7/7	16:50	3,341.660	15,603.64	4,172.874
7/8	17:32	5,927.785	6,471.466	8,215.726

Aerosol Recirculation

Based on Fig. 3 alone it is not clear if there are any reticulation effects present. Thus, we can also look at each day individually within our consecutive period.

Here it is not immediately evident that we seeing strong recirculation effects. We do observe aerosol content increasing consistently between days 3-5 however, over the full 6 day consecutive period there is not a consistent linear increase. Though if we only consider the starting and ending value, we do see a general increase in aerosols from the start of the period to the end of the period, supporting the notion that multi-day SB events may contribute to worsening air quality events.

When looking at it broken down by time of day, there appears to be an overall upward trend in the morning and post-SB aerosol content. Breaking this down by hour shows us that in addition to the peak after SB passage, the aerosol content spikes at sunrise, and generally only after the first day. One theory suggests that this spike could be associated with some local anthropogenic source that only occurred on particular days. Unfortunately, without more consecutive SB cases, it is hard to investigate this simple theory further.

However, another theory may suggest that this spike may be associated with the presence of secondary aerosol generation as the result of photochemical reactions taking place around sunrise. The increased presence of secondary aerosols was seen in simulations done by Talbot et al. (2007) for multiple days of SB passage. With more time we could analyze data from other instruments at ARM-AMF1 that have the capabilities to return aerosol composition and size distribution to determine if the present particles underwent chemical makeup and size changes after sunrise, or if they were transported in.

Boundary Layer Structure

With an increase in aerosol content near the surface near the time of SB passage we should also expect the height of the CBL to decrease with the passage of the SB (Miller et al. 2003), and vertical mixing to suppress (Ohba

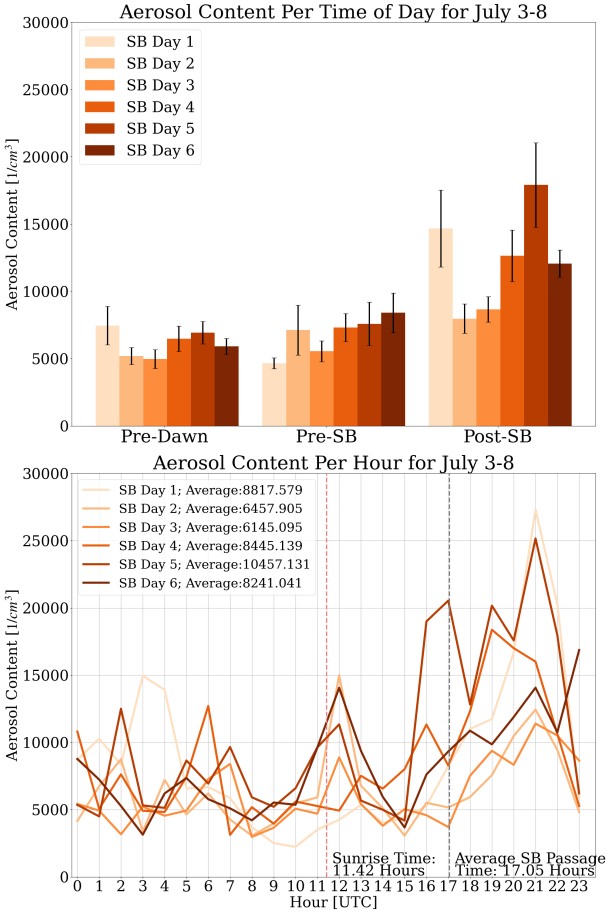

FIG. 4. Time of day (pre-dawn, pre-SB, post-SB) averaged aerosol content per consecutive SB day (top),and hourly averaged aerosol content for consecutive SB days(bottom), with orange colors darkening with days into the consecutive period. Error bars are denoted on the top figure for each bar. In the bottom figure the average time of SB passage is noted and marked with a grey dashed line, the sunrise time is noted and marked with a light red dashed line, and the overall average value of aerosol content is also calculated and noted in the figure legend for each day in the consecutive period.

et al. 1998; Dewani et al. 2023). In Fig. 5 we observe in both single and consecutive cases the ABL height lowers after the passage of the SB, much sooner than the diurnal cycle suggests. In both cases there is also a small rebound in ABL height, such that the layer begins growing again slightly before the early evening transition. This trend is more noticeable in the consecutive cases

The nighttime stable layer is also drastically lower for both SB cases compared to the clear cases. Looking at the clear cases individually, these estimates seem to be elevated by the presence of deep nocturnal inversions in the mid-June cases.

Here we also see a decrease in σ_w^2 within the ABL on days with SB passage. This supports the wind tunnel experiments of Ohba et al. (1998), which notioned that SB

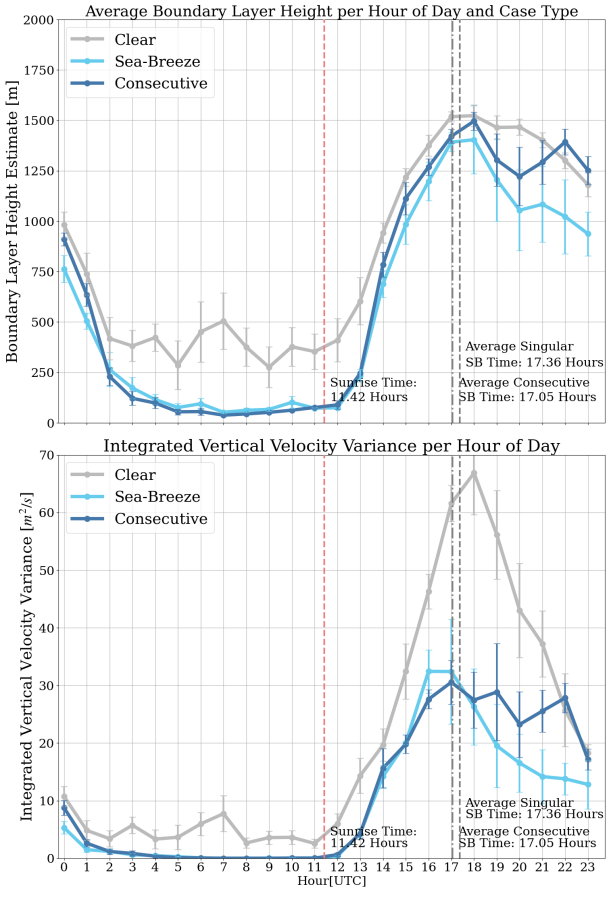

FIG. 5. ABL Height estimates (top) and vertically integrated σ_w^2 (bottom) integrated over the depth of the ABL for clear cases (grey), singular SB cases (light blue), and consecutive SB cases (dark blue), with respective average SB passage time marked (dashed grey) and sunrise time marked (light red).

passage would suppress vertical buoyant transport leading to an increase in surface aerosol content. This decrease is not confined to post-SB passage, as the early morning hours show noticeably lower values of σ_w^2 compared to the clear case. This may further explain why we saw decreases in daytime aerosol content before SB passage time in the clear cases and not the SB cases.

5. Conclusions

Overall our findings are consistent with prior literature, such that the passage of the SB correlated with an average increase in aerosol content when compared to days with out SBs. This finding carried for days with different timings fo the SB, over a two month period. This also further supports the idea that in additional to aerosol transport, the SB helps to suppress the vertical mixing of the daytime CBL, as shown in decreases of σ_w^2.

To further this work, it would be important to investigate the chemical makeup of the present aerosols to quantify the effects of recirculation on secondary particle generation. To support this notion, more consecutive cases would also be needed to ensure this period represents a typical consecutive case and does not have additional signal from local anthropogenic forcing that may have occurred only during this period.

Going forward, using the co-located University of Oklahoma Coptersonde and University of Colorado RAAVEN at the Brazoria wildlife refuge south of Houston could give additional insight into the effects of SB passage. It would also be useful to use data from both the flight locations and AMF1 site to investigate the effects of both advection and buoyancy suppression on aerosol content. If the data from these flights are not used, finding another site to obtain aerosol information to accomplish the same analysis would be extremely useful.

Acknowledgments. This work was completed as a project for Professor Julie Lundquist's energy meteorology class at Johns Hopkins University. The authors acknowledge the insights, support, and encouragement from Professor Lundquist and F. Başak Rakici of Johns Hopkins University.

Data availability statement. The observational data used for this project is publicly available through the Atmospheric Radiation Measurement (ARM) database at https://adc.arm.gov/discovery/#/results/site_code::hou. The data products used include *aoscpcf* (2.5 nm CPC), *dlfpt*, *profwind4news* (lidar stares and derived horizontal winds respectively), *mwrlos*, and *tropoe* (line of sight and tropospheric optimal estimation retrieval (TROPOE) from MWR respectively).

Additionally, the code used for this project is hosted in a GitHub repository at https://github.com/IMedina-WxMech/TRACER_Data_Analysis/. This contains code for SB identification, data analysis, and a modified version of the Smith and Carlin (2024) fuzzy-logic code. The repository also includes some of the data used that was not too large to upload.

References

Augustin, P., and Coauthors, 2020: Impact of sea breeze dynamics on atmospheric pollutants and their toxicity in industrial and urban coastal environments. *Remote Sensing*, **12 (4)**, 648, doi:10.3390/rs12040648, URL https://www.mdpi.com/2072-4292/12/4/648, publisher: Multidisciplinary Digital Publishing Institute.

Chen, F., S. Miao, M. Tewari, J.-W. Bao, and H. Kusaka, 2011: A numerical study of interactions between surface forcing and sea breeze circulations and their effects on stagnation in the greater houston area. *J. Geophys. Res.*, **116**, D12 105, doi:10.1029/2010JD015533, URL http://doi.wiley.com/10.1029/2010JD015533.

Dewani, N., M. Sakradzija, L. Schlemmer, R. Leinweber, and J. Schmidli, 2023: Dependency of vertical velocity variance on meteorological conditions in the convective boundary layer. *Atmospheric Chemistry and Physics*, **23 (7)**, 4045–4058, doi:10.

5194/acp-23-4045-2023, URL https://acp.copernicus.org/articles/23/4045/2023/.

Jensen, M., and Coauthors, 2023: DOE/SC-ARM–23-038, 2202672. Tracking aerosol convection interactions experiment (TRACER) field campaign report. URL https://www.osti.gov/servlets/purl/2202672/, DOE/SC–ARM–23–038, 2202672 pp., doi:10.2172/2202672.

Klein, P., E. Smith, T. Wagner, J. Gibbs, T. Bell, J. Gebauer, M. Spencer, and M. Carney, 2023: DOE/SC–ARM-23-027, 1984939. TRACER-coastal urban boundary-layer interactions with convection (TRACER-CUBIC) field campaign report. URL https://www.osti.gov/servlets/purl/1984939/, DOE/SC–ARM–23–027, 1984939 pp., doi:10.2172/1984939.

Lappin, F., T. Bell, P. Klein, and G. d. Boer, 2025: Quantifying the thermodynamic impacts on the atmospheric boundary layer due to the sea breeze in the coastal houston region. *Journal of Applied Meteorology and Climatology*, **64 (6)**, doi:10.1175/JAMC-D-24-0203.1, URL https://journals.ametsoc.org/view/journals/apme/64/6/JAMC-D-24-0203.1.xml, section: Journal of Applied Meteorology and Climatology.

Miller, S. T. K., B. D. Keim, R. W. Talbot, and H. Mao, 2003: Sea breeze: Structure, forecasting, and impacts. *Reviews of Geophysics*, **41 (3)**, 2003RG000 124, doi:10.1029/2003RG000124, URL https://agupubs.onlinelibrary.wiley.com/doi/10.1029/2003RG000124.

Moorthy, K. K., B. V. K. Murthy, and P. R. Nair, 1993: Sea-breeze front effects on boundary-layer aerosols at a tropical coastal station. *Journal of Applied Meteorology*, **32**, URL https://journals.ametsoc.org/view/journals/apme/32/7/1520-0450_1993_032_1196_sbfeob_2_0_co_2.xml, section: Journal of Applied Meteorology and Climatology.

Ohba, R., Y. Shao, and A. Kouchi, 1998: A wind tunnel and numerical investigation of turbulent dispersion in coastal atmospheric boundary layers. *Boundary-Layer Meteorology*, **87 (2)**, 255–273, doi:10.1023/A:1000941406502, URL https://doi.org/10.1023/A:1000941406502.

Parajuli, S. P., G. L. Stenchikov, A. Ukhov, I. Shevchenko, O. Dubovik, and A. Lopatin, 2020: Aerosol vertical distribution and interactions with land/sea breezes over the eastern coast of the red sea from lidar data and high-resolution WRF-chem simulations. *Atmospheric Chemistry and Physics*, **20 (24)**, 16 089–16 116, doi:10.5194/acp-20-16089-2020, URL https://acp.copernicus.org/articles/20/16089/2020/, publisher: Copernicus GmbH.

Physick, W. L., and R. a. D. Byron-Scott, 1977: Observations of the sea breeze in the vicinity of a gulf. *Weather*, **32 (10)**, 373–381, doi:10.1002/j.1477-8696.1977.tb04481.x, URL https://onlinelibrary.wiley.com/doi/abs/10.1002/j.1477-8696.1977.tb04481.x, _eprint: https://rmets.onlinelibrary.wiley.com/doi/pdf/10.1002/j.1477-8696.1977.tb04481.x.

Smith, E. N., and J. T. Carlin, 2024: A multi-instrument fuzzy logic boundary-layer-top detection algorithm. *Atmospheric Measurement Techniques*, **17 (13)**, 4087–4107, doi:10.5194/amt-17-4087-2024, URL https://amt.copernicus.org/articles/17/4087/2024/, publisher: Copernicus GmbH.

Talbot, C., P. Augustin, C. Leroy, V. Willart, H. Delbarre, and G. Khomenko, 2007: Impact of a sea breeze on the boundary-layer dynamics and the atmospheric stratification in a coastal area of the north sea. *Boundary Layer Meteorology*, **125 (1)**, 133–154, doi:10.1007/s10546-007-9185-6, URL https://www.proquest.com/docview/738387890/abstract/2A11001866AD4006PQ/1, num Pages: 133-154 Place: Dordrecht, Netherlands Publisher: Springer Nature B.V.

Wang, D., R. Kobrosly, T. Zhang, T. Subba, S. van den Heever, S. Gupta, and M. Jensen, 2025: Aerosol impacts on isolated deep convection: findings from TRACER. *Atmospheric Chemistry and Physics*, **25 (16)**, 9295–9314, doi:10.5194/acp-25-9295-2025, URL https://acp.copernicus.org/articles/25/9295/2025/, publisher: Copernicus GmbH.